Vinyl ethylene sulfite as a new additive in propylene carbonate-based electrolyte for lithium ion batteries

Wanhao Yao,[a] Zhongru Zhang,[a] Jun Gao,[a] Jie Li,[a] Jie Xu,[b] Zhoucheng Wang[b] and Yong Yang*[a]

Received 13th March 2009, Accepted 19th June 2009
First published as an Advance Article on the web 17th July 2009
DOI: 10.1039/b905162g

Vinyl ethylene sulfite (VES) is studied as a new additive in propylene carbonate (PC)-based electrolyte for lithium ion batteries. The electrochemical results show that the artificial graphite material exhibits excellent electrochemical performance in a PC-based electrolyte with the addition of the proper amount of VES. According to our spectroscopic results, VES is reduced to $ROSO_2Li$ ($R{=}C_4H_6$), Li_2SO_3 and butadiene (C_4H_6) through an electrochemical process which precedes the decomposition of PC. Furthermore, some of the Li_2SO_3 could be further reduced to Li_2S and Li_2O. All of these products are proven to be components of the solid electrolyte interface (SEI) layer.

1. Introduction

Lithium ion batteries have the merits of a non-memory effect, high working cell voltage, low environmental pollution, low self-discharge rate, and high specific energy density. They have already been successfully used as a secondary source in laptop communications, and consumer electronic productions in daily life. In the near future, they may also help fight global warming by improving the performance of electric- or hybrid-vehicles which have zero or reduced carbon emissions.[1]

The electrolyte is a very important component for lithium ion batteries, it can not only influence the electrochemical performance greatly, but also affect the safety of the batteries. With the excellent properties of low melting point, high boiling point, high flash point, high chemical stability toward metallic lithium and a wide electrochemical window, propylene carbonate (PC) is an attractive candidate as a solvent for nonaqueous electrolyte in lithium ion batteries.[2] However, PC is not suitable for a graphitic anode due to its tendenency to intercalate into graphite during the first charge process which leads to the destruction of the graphite structure.[3–6] Therefore, many methods have been developed to solve this problem. One effective method is the employment of film-forming electrolyte additives which are reduced predominantly on the graphite electrode surfaces during the first cycling process. These additives mainly include some functional groups such as vinylene compounds and sulfite. For example, vinylene carbonate (VC)[7] and vinyl ethylene carbonate (VEC),[8,9] which have a vinylene group, have been studied as additives for PC-based electrolyte. They play an important role in the protection of the structure of the graphitic anode from destruction by PC, but they also have some shortcomings—the VC additive is known to be an unstable compound because of polymerization. With VEC, there was no effective SEI layer to prevent the intercalation of PC into MesoCarbon MicroBeads (MCMB) in a PC-based electrolyte with 5 wt% VEC at a low current density.[9] Meanwhile, as a novel solvent or electrolyte additive, sulfites have been attracting increased attention. Winter *et al.*[10] have reported on the use of cyclic organic sulfites, ethylene sulfite (ES) as a film-forming electrolyte additive in a PC-based electrolyte for lithium ion batteries with graphitic anode. ES in only 5% presence successfully eliminated the exfoliation of the graphite anode, and prevented the irreversible process of reduction of ES which occurs at 2.0 V. However, the decomposition potential of ES on the cathode material is less than 3.5 V, so it is unstable in a practical cell.[11] Chen *et al.*[12] have synthesized another film-forming additive butylene sulfite (BS) which can help realize the graphite anode and enable $LiMn_{1.99}Ce_{0.01}O_4$ or $LiFePO_4$–C cathodes battery systems to work in PC-based electrolyte. However, the coulombic efficiency of the first cell

Broader context

Lithium ion batteries have an important role in energy storage applications, and they may also help fight global warming by improving the performance of electric- or hybrid-vehicles, which have zero or reduced carbon emissions. Propylene carbonate (PC) is an attractive candidate as a solvent for nonaqueous electrolytes in lithium ion batteries, however, it is not suitable for the graphitic anode due to its tendency to intercalate into graphite during the first charge process, which leads to the destruction of the graphite structure. Here, we put forward a new film-forming additive, vinyl ethylene sulfite (VES), which has two functional groups—a sulfite group and a vinylene group—which shows better electrochemical performance than some other additives, and offers the possibility of using PC in lithium ion batteries with graphite as the anode.

---

[a] *State Key Laboratory for Physical Chemistry of Solid Surfaces & Department of Chemistry, College of Chemistry and Chemical Engineering, Xiamen University, Xiamen, 361005, PR China. E-mail: yyang@xmu.edu.cn; Fax: +86-592-2185753; Tel: +86-592-2185753*
[b] *Department of Chemical and Biochemical Engineering, College of Chemistry and Chemical Engineering, Xiamen University, Xiamen, 361005, PR China*

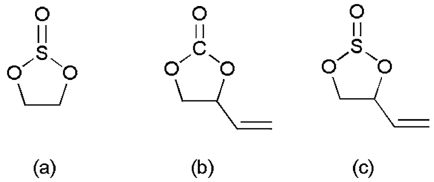

Fig. 1 Structural formulae of (a) ethylene sulfite (ES), (b) vinyl ethylene carbonate (VEC), and (c) vinyl ethylene sulfite (VES).

cycle with additive BS is less than 50%, which limits its application in practical cells. In summary, these additives which have different functional groups like a sulfite group or vinylene group, have been proven to prevent the intercalation of PC into the graphitic anode to some degree, but they also have their own disadvantages.

In this paper, we put forward a new film-forming additive, vinyl ethylene sulfite (VES). It has a similar molecular structure to VEC and ES (Fig. 1), while providing both a sulfite group and vinylene group in a molecule, so it is expected to show better electrochemical performance with the combined effects of pure VEC or ES additives. In our work, the electrochemical performance of the graphitic anode in PC-based electrolytes with and without VES was investigated systematically, the composition of the SEI layer on the surface of graphite was analyzed and the possible active mechanism of VES additive was proposed according to our spectroscopic results.

2. Experimental

2.1 Preparation of electrolyte

VES ($C_4H_6SO_3$) (Fujian Chuangxin Science and Technology Develops Co. Ltd, Fuzhou, China) was stored over 4 Å molecular sieves under high purity argon, and $LiClO_4$ was dried at 120 °C vacuum for 10 h. Electrolyte solutions were prepared by dissolving stoichiometric $LiClO_4$ into the mixture solvents in a dry glove box filled high purity argon (Labmaster100, Mbraun, Germany). All solvent ratios indicated in this paper are in volume ratios.

2.2 Electrochemical measurement

The graphite electrode was prepared by slurrying the artificial graphite (CAG) powder (Shanshan Co. Ltd, Dongguan, China) with 5 wt% carbon black and 10 wt% polyvinylidene fluoride (PVDF). The slurry was spread onto a copper foil and dried at 80 °C under vacuum for 6 h. Constant current charge/discharge experiments were carried out on battery testers (Land CT2001A) by coin cells at room temperature, the lithium metal (99.9%) was used as the counter electrode. The cell was cycled between 0.005 V and 2.0 V at a current density of 37 mA g^{-1}.

Cyclic voltammetry (CV) measurements were performed with the same coin cells on a CHI604 electrochemical workstation (Chenhua Instrument Co. Ltd, Shanghai, China) with lithium metal as the counter and reference electrode at a scan rate of 0.1 mV s^{-1}. All the cells were assembled under a dry argon atmosphere in the glove box.

2.3 *In-situ* differential electrochemical mass spectrometry (DEMS)

In-situ Differential Electrochemical Mass Spectrometry (DEMS) setup used has been described in a previous work.[13] It consisted of a quadrupole mass spectrometer (Aeolos QMS 403 C, Netzsch, Germany) and an electrochemical cell. The working electrode was made by blade-coating the CAG slurry on a copper net, the counter and reference electrodes were lithium metals. All DEMS tests were carried out potentiodynamically, and the cutoff voltages for cyclic voltammetry (CV) were 2.0 V and 0.005 V with a scan rate of 0.1 mV s^{-1}.

2.4 SEI analysis

SEI analyses of the CAG surface used two different electrodes from the coin-cell battery test, including one charged to 0.005 V in 1 M $LiClO_4$/PC + VES (80 : 20) and the other charged for 10 h in 1 M $LiClO_4$/PC. The CAG electrodes were removed from the coin-cell battery and rinsed with anhydrous PC (Shanshan Co. Ltd, Dongguan, China) in the glove box, then left in the glove box for 24 h to make sure they were dry. Scanning electron microscopy (SEM) (Oxford Company LEO1530) equipped with an energy dispersive spectroscope (EDS) detector was used to inspect the surface morphology of the electrodes. The X-ray photoelectron spectroscopy (XPS) analysis was performed using a Quantum 2000 ESCA spectrometer (Physical Electronics, USA) with monochromatic Al Kα 1486.6 eV radiation operated at 23.2 W in a vacuum of $<10^{-8}$ Torr. The binding energy was calibrated with reference to the C 1s level of hydrocarbon (284.6 eV).

2.5 Theoretical calculations

All the calculations had been performed using the Gaussian 03 program package.[14] The geometry optimizations of the organic carbonates and sulfites were carried out with the DFT models and B3PW91 method with 6–311 + G(d, p) basis set.[15] Besides that, the total energy and frontier molecular orbital energy of each organic molecule were also calculated.

3. Results and discussion

3.1 DFT calculations

Table 1 shows total energy and frontier molecular orbital energy of VES and PC. It can be seen that the energy level of lowest unoccupied molecular orbital (LUMO) of VES is much lower than that of PC solvent. Based upon molecular orbital theory, a molecule with a lower energy level of LUMO should be a better

Table 1 Total energy and frontier molecular orbital energy of PC and VES

		Frontier molecular orbital energy/Ha		
Organic molecule	E_T/Ha	E_{HOMO}	E_{LUMO}	$\Delta E_g{}^a = E_{LUMO} - E_{HOMO}$
PC	−381.6863	−0.3066	−0.0123	0.2943
VES	−779.7462	−0.2945	−0.0471	0.2474

electron acceptor and more reactive on the negatively charged surface of the anode. Therefore, VES will be reduced prior to PC solvent during the first charge process. The theoretical calculations are consistent with the experimental results.

3.2 Charge/discharge cycles

Fig. 2 shows the first charge/discharge profiles of the CAG/Li cells in electrolytes containing different content of VES. In curve (A) without VES, the potential drops rapidly and then keeps constant at about 0.90 V, at which point PC solvent decomposition and exfoliation of CAG take place ceaselessly. Thus, the lithium ion would not intercalate into the CAG electrode because the intercalation should happen at a potential below 0.25 V.[8] In curve (B) with 1 M $LiClO_4$/PC + VES electrolyte (98 : 2), there is a reductive plateau at 1.46 V which is attributed to the reduction of VES. However the long charge plateau still exists with this content of VES, and the potential 0.86 V is lower than that in 1 M $LiClO_4$/PC. When the electrolyte contains 5% VES (curve (C)), the reduction of VES increases to 1.51 V, and the long charge plateau decreases to 0.80 V. If the VES content is increased to 10%, the voltage profile changes significantly and two reductive plateaux emerge, as shown in curve (D), one at 1.56 V is attributed to the reduction of VES, and the other at 0.79 V is ascribed to solvent intercalation into graphite. It is important to see a charge/discharge plateau below 0.25 V appear, this is attributed to the intercalation and deintercalation of lithium ion, indicating that the charge/discharge process is realized. Different from curve (D), in curve (E) there exist only two plateaux, one for 20% VES in electrolyte which is located at 1.64 V, and the other is below 0.25 V. The plateau at 0.79 V which is ascribed to the solvent intercalation into graphite disappears. Therefore, solvent intercalation can be prevented in the electrolyte with proper content of VES, *e.g.* 20%. In this type of electrolyte, PC decomposition and CAG exfoliation can be suppressed significantly during electrochemical intercalation of lithium ions.

Fig. 3 shows the cycle performance of CAG/Li cells in the electrolyte with different concentrations of VES. It can be seen that the first charge/discharge capacity of the cell with 10% VES is only 301.4 mAh g^{-1}/184.3 mAh g^{-1}, and the reversible capacity can increase to 279 mAh g^{-1} after the sixth cycle. However, the first charge and discharge capacity of the cell with 20% VES reached up to 386.2 mAh g^{-1} and 298.5 mAh g^{-1}, and the reversible capacity increased to 314.0 mAh g^{-1} at the fourth cycle, which is much better than that of the cell with pure additive VEC[9] or ES.[11] In addition, the coulombic efficiency of the first cycle for the cell with 10% VES is only 61.2%, but it can increase to 77.3% when the concentration of VES reaches to 20%. Also, the cycle stability of the cell with 20% VES is better than that of 10% VES which proves that the addition of VES is positive for the cycle life of batteries. All of these phenomena indicate that a 20% volume percentage is the proper choice for VES as an electrolyte additive for lithium ion batteries.

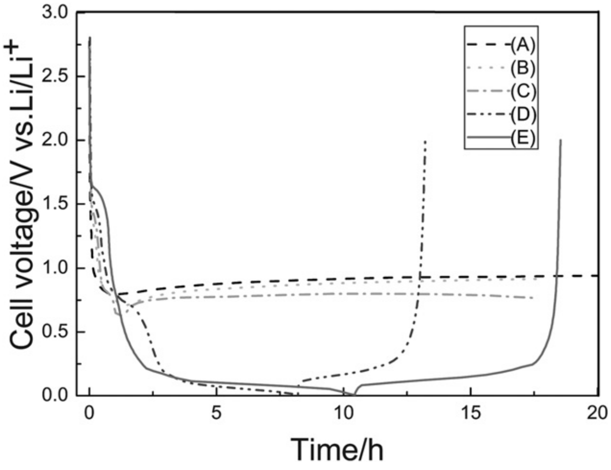

Fig. 2 The first charge/discharge voltage profiles of the CAG/Li half-cell in 1 M $LiClO_4$/PC electrolytes with different volume content of VES cycled between 2.0–0.005 V at 37 mA g^{-1} and current density: (A) 0%, (B) 2%, (C) 5%, (D) 10%, and (E) 20%.

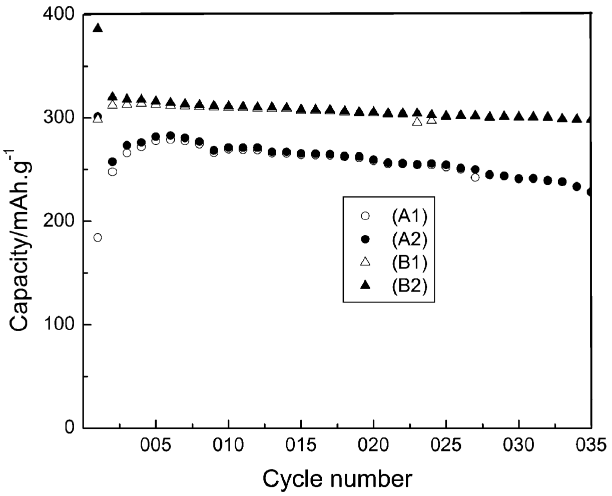

Fig. 3 Cycle performances of CAG/Li cells in two kinds of electrolytes, (A1) and (A2) 1 M $LiClO_4$/PC + VES (90 : 10), (B1) and (B2) 1 M $LiClO_4$/PC + VES (80 : 20). (○,△) discharge capacities, (●,▲) charge capacities. Current density = 37 mA g^{-1}, cutoff voltage = 2.0–0.005 V *vs* Li/Li^+.

3.3 Cyclic voltammetry measurements

The electrochemical decomposition process of VES additive was investigated by CV measurements. Fig. 4 shows the CV curves of CAG electrode in 1 M $LiClO_4$/PC electrolyte, 1 M $LiClO_4$/PC + VES (90 : 10) electrolyte and 1 M $LiClO_4$/PC + VES (80 : 20) electrolyte, respectively. In Fig. 4a, there is a small peak at 0.75 V and large irreversible peak around 0.46 V *vs* Li/Li^+ on the first cathodic sweep, the former can be attributed to the decomposition of PC, and the latter comes from the exfoliation of graphite as a result of PC decomposition.[7] The larger peak which still exists in the second cycle shifts to a higher potential range. In Fig. 4b, the peak at 0.46 V becomes almost undiscernible, and the intensity of the peak at 0.75 V becomes lower. A new peak at 1.48 V emerges, which can be attributed to the reduction of VES. This result which is the same as that of cycle performance proves that the decomposition of PC can be prevented under the representation of VES, and that exfoliation of graphite can also be suppressed. Thus we propose that a stable SEI layer on the surface of CAG is formed during the electrochemical process after VES is added. When the concentration of VES in the

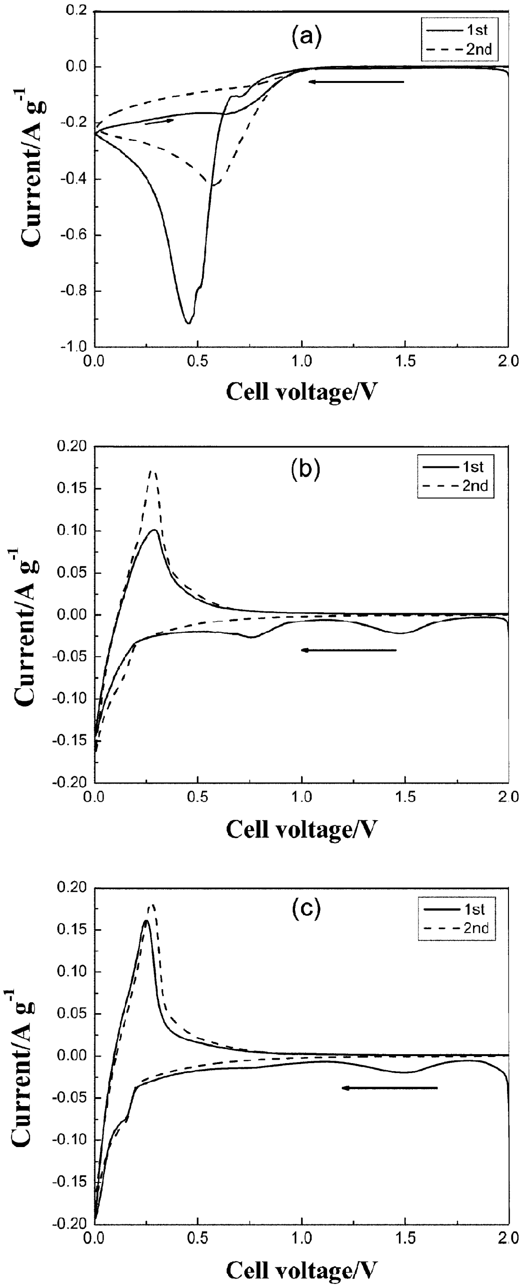

Fig. 4 Cyclic voltammograms of CAG electrode in (a) 1 M $LiClO_4$/PC, (b) 1 M $LiClO_4$/PC + VES (90 : 10), and (c) 1 M $LiClO_4$/PC + VES (80 : 20) with a scan rate of 0.1 mV s^{-1}.

electrolyte increases to 20% (Fig. 4c), there are still two reductive peaks at the same voltage as on the first cathodic sweep curve in Fig. 4b, but the one at 0.76 V has almost disappeared, this indicates that the SEI layer on the surface of CAG in 1 M $LiClO_4$/PC + VES (80 : 20) electrolyte is much better than the one with 10% VES. In addition, in Fig. 4b or Fig. 4c, the two reductive peaks at 1.48 V and 0.76 V disappear in the second cycle, which indicates that the SEI layer on the surface of CAG was completely formed during the first cycle. The improvement of electrochemical performance of the CAG electrode should therefore benefit from the decomposition product of VES.

3.4 SEM and EDS analysis of the electrodes

Fig. 5 shows SEM images of the surface of CAG electrodes which were charged in 1 M $LiClO_4$/PC electrolyte with or without VES. Prior to cycling (Fig. 5(a3)), the surface of the original CAG is smooth. After charging for ten hours in pure 1 M $LiClO_4$/PC electrolyte (Fig. 5(b3)), it can be seen that the surface of CAG is rough and that there is some exfoliation of CAG material, which indicate that the structure of the CAG electrode is destroyed. Contrary to this, the morphology of the electrode charged to 0.005 V in electrolyte with 20% VES (Fig. 5(c3)) is unchanged, the surface is smooth and no exfoliation of CAG is observed. Thus, VES is proposed to play an important role in suppressing the decomposition and intercalation of PC into the CAG electrode, and of protecting the structure of CAG in PC-based electrolytes.

In order to understand the composition formed on the CAG surface, the CAG electrode, after the first cycle in electrolyte with 20% VES added, was analyzed with EDS. The result is shown in Fig. 6. A sulfur peak at 2.3 keV was detected on the CAG surface. It is apparent that this peak corresponds to sulfur in the sulfite compounds formed on the CAG electrode surface during the reduction of VES. This suggests that the reductive products of VES take part in the formation of the SEI layer.

3.5 *In-situ* differential electrochemical mass spectrometry (DEMS)

We know some small molecular gases always emerge from the decomposition of electrolyte during the charge/discharge process in lithium ion batteries. Differential Electrochemical Mass Spectrometry (DEMS) has been proven to be very useful for studying gas evolution,[13,16] so information was obtained about the electrochemical behavior of electrolyte after the addition of VES using this method.

Fig. 7a show results of DEMS analysis of the CAG/$LiClO_4$ (1 M) + PC/Li cell during the cyclic potential sweeping process. The peaks at m/z signals of 42 and 41 can be assigned to evolved propylene (C_3H_6).[16] The onset voltage for evolution of C_3H_6 is around 0.86 V *vs* Li/Li$^+$. Corresponding to the decomposition of PC (see Fig. 4), C_3H_6 should come from the decomposition of PC, a result proved by M. R. Wagner *et al.*[16] Thus the problem of graphitic anodes in pure PC-based electrolyte can be attributed to the decomposition of PC and the formation of propylene gas. This would cause the graphite particles to exfoliate and crack. When 10% VES or 20% VES is added, the peaks for evolved C_3H_6 are significantly decreased, and disappear totally in the profile for 20% VES. That is to say the decomposition of PC can be prevented by adding VES. VES decomposes before PC, and the VES decomposition products help build up a good SEI layer on the surface of the CAG electrode, greatly improving cycle performance.

On other hand, the signals at m/z 54 and m/z 53 with similar peak profiles were detected (see Fig. 7b and 7c) and assigned to butadiene (C_4H_6). The only difference between Fig. 7b and 7c is that the onset potential of butadiene (m/z 53 and m/z 54) with 20% VES is about 1.71 V which is higher than that found for 10% VES at 1.66 V. This is consistent with former CV results. However, the signals at m/z 54 and m/z 53 were not detected in pure PC-based electrolyte. Thus, the butadiene gas detected must

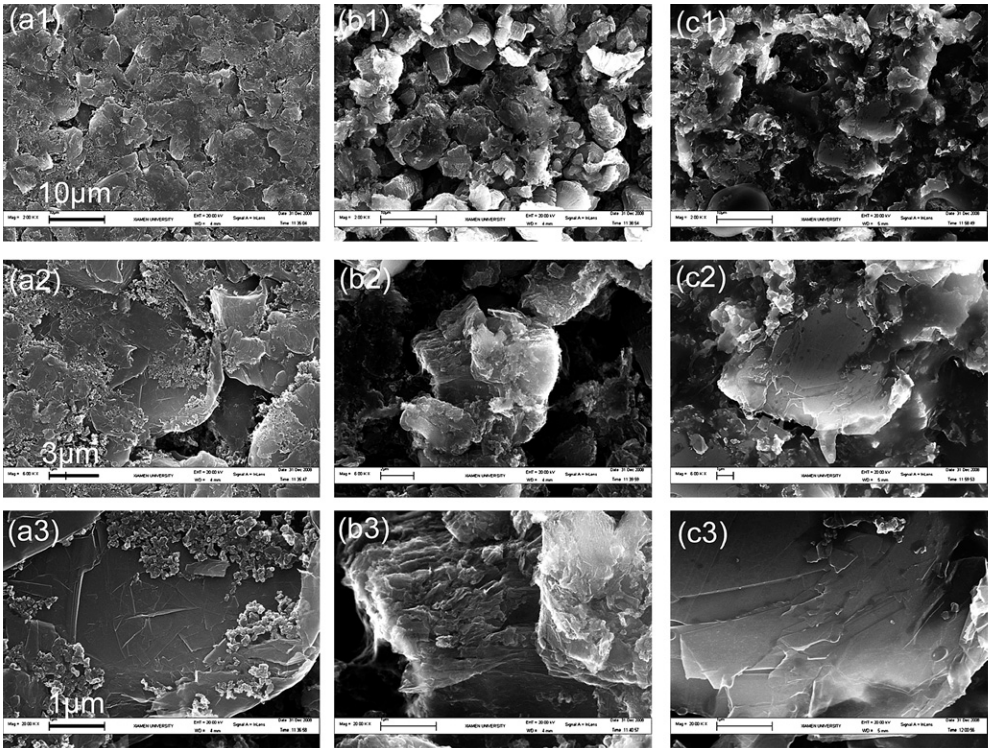

Fig. 5 SEM images of CAG electrode surface obtained (a) before charging, (b) after charging for ten hours in 1 M $LiClO_4$/PC, and (c) after the first charge to 0.005 V in 1 M $LiClO_4$/PC + VES (80 : 20). Magnification: ×2000 (a1) (b1) (c1): ×6000 (a2) (b2) (c2); ×20000 (a3) (b3) (c3).

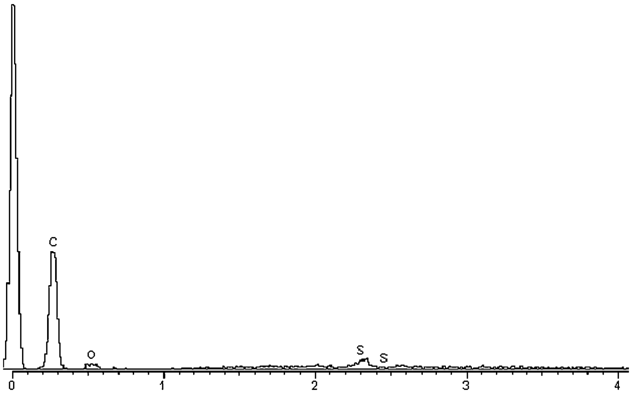

Fig. 6 EDS of CAG electrode after the first charge to 0.005 V in 1 M $LiClO_4$/PC + VES (80 : 20).

have come from the electrochemical reduction of VES. In addition, the signal at m/z 64 assigned to SO_2 is not detected, which indicates that SO_2 is not a reduction product of VES. Based on the results of DEMS and XPS analyses the reductive process of VES is presented in eqn (1):

$$\begin{aligned} \text{VES } (C_4H_6SO_3) + 2Li^+ + 2e^- &\rightarrow Li_2SO_3 \\ &+ CH_2{=}CH\text{–}CH{=}CH_2\uparrow \end{aligned} \tag{1}$$

3.6 XPS analysis of the electrode

Fig. 8a shows the S2p XPS spectra with curve fitting of the CAG electrode charged to 0.005 V in 1 M $LiClO_4$/PC + VES (80 : 20) electrolyte. The peaks around 168 eV–169 eV were assigned to Li_2SO_3 and $ROSO_2Li$, and the peak at 161.5 eV was considered to be Li_2S.[17,18] All of these compounds were proposed to be the main components of the SEI layer. O1s spectra of the anode is shown in Fig. 8b. The broad peak between 529 eV and 535 eV may include Li_2SO_3 and $ROSO_2Li$. The other peak at 528.7 eV can be assigned to Li_2O.[19] Compared with the S2p XPS spectra, beside Li_2SO_3, $ROSO_2Li$ and Li_2S, Li_2O was also a component of the SEI layer. According to the XPS results of S2p and O1s, we consider that some of Li_2SO_3 may further decompose to Li_2S and Li_2O, which is expressed by eqn (2).

$$Li_2SO_3 + 6Li^+ + 6e^- \rightarrow Li_2S + 3Li_2O \tag{2}$$

4. Conclusions

A new additive, vinyl ethylene sulfite (VES) whose structure combines the functional groups sulfite and vinylene was investigated in PC-based electrolyte for lithium ion batteries with graphitic anode. The CAG electrode showed excellent electrochemical performance in the electrolyte with 20% VES added, a better performance than that obtained with electrolytes containing only VEC or ES. This improvement was attributed to the newly formed compact SEI layer from reduction of VES which suppressed the intercalation of the PC molecule. During the first charge process, VES may be reduced to $ROSO_2Li$, Li_2SO_3 and C_4H_6 by an electrochemical route, and the Li_2SO_3 formed may generate Li_2S and Li_2O. This provides the possibility for PC to be

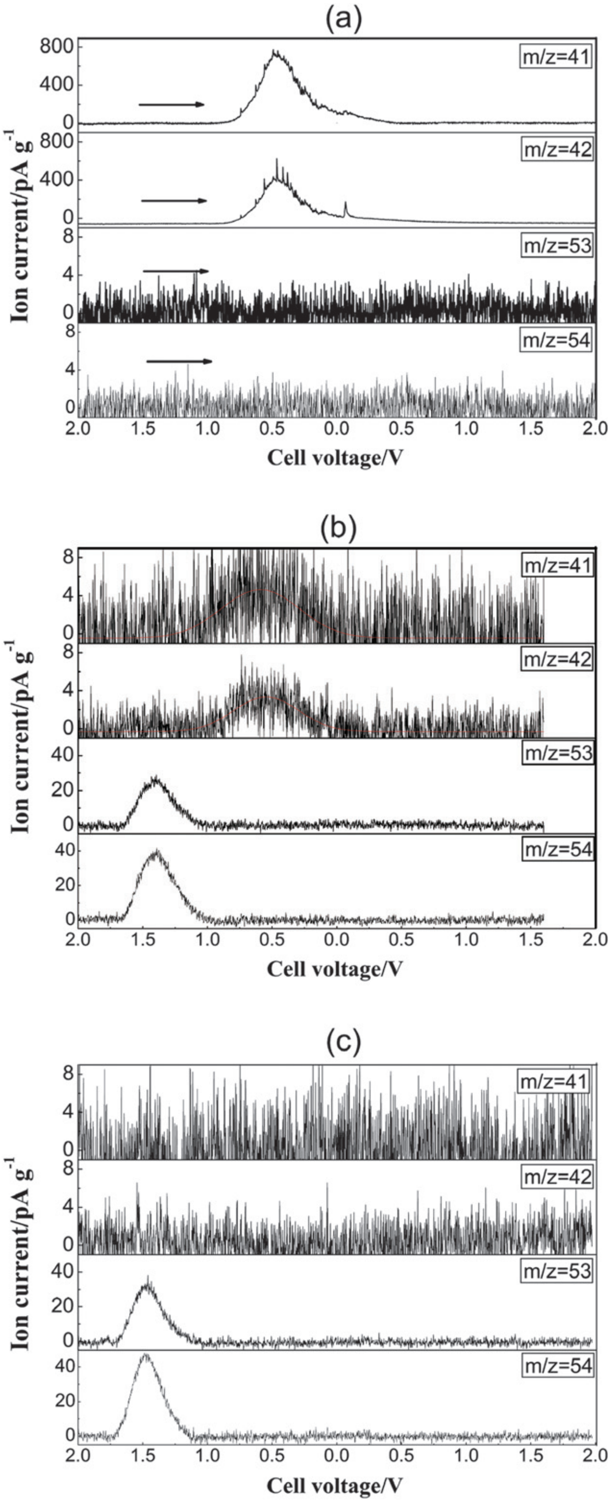

Fig. 7 Comparative plot of *m*/*z* signal intensities as a function of cell voltage for a typical CAG electrode in (a) 1 M $LiClO_4$/PC, (b) 1 M $LiClO_4$/PC + VES (90 : 10) and (c) 1 M $LiClO_4$/PC + VES (80 : 20). Scan rate: 0.1 mV s^{-1}.

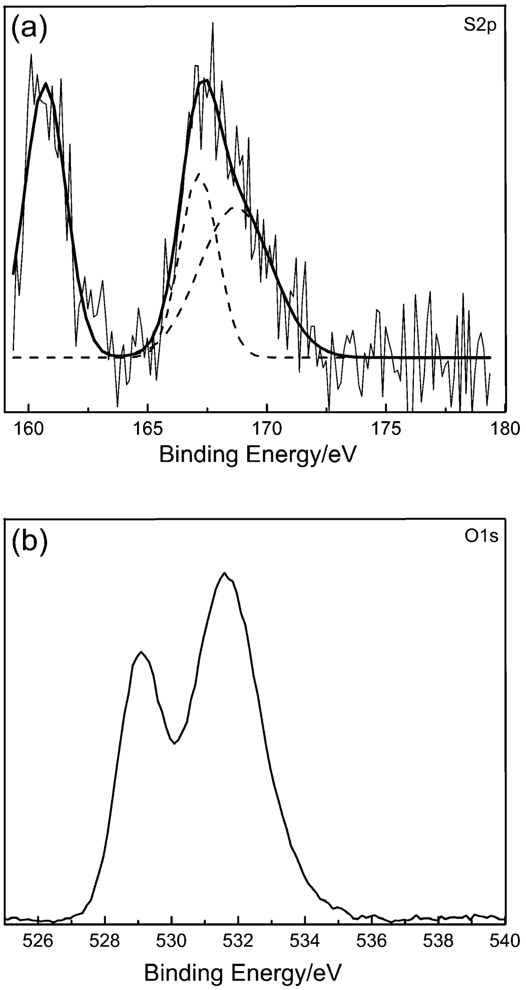

Fig. 8 S2p and O1s XPS spectra of CAG electrode charged to 0.005 V in 1 M $LiClO_4$/PC + VES (80 : 20).

used as an electrolyte solvent in lithium ion batteries with graphite as the anode.

Acknowledgements

This work was supported by the National Natural Science Foundation of China (NNSFC, Grant No.29925310, 20433060, 20473068) and National Basic Research Program of China (973 Program) (Grant No. 2007CB209702) from Ministry of Science and Technology, China. We are also grateful to Fujian Chuangxin Science and Technology Develops Ltd (Fuzhou) for providing the additive used in this study.

References

1 B. Scrosati, *Nat. Nanotech.*, 2007, **2**, 598–599.
2 J. T. Lee, Y. W. Lin and Y. S. Jan, *J. Power Sources*, 2004, **132**, 244–248.
3 D. Aurbach, A. Zaban, Y. Ein-Eli, I. Weissman, O. Chusid, B. Markovsky, M. Levi, E. Levi, A. Schechter and E. Granot, *J. Power Sources*, 1997, **68**, 91–98.
4 M. Fujimoto, Y. Shoji, Y. Kida, R. Ohshita, T. Nohma and K. Nishio, *J. Power Sources*, 1998, **72**, 226–230.
5 H. Kaneko, K. Sekine and T. Takamura, *J. Power Sources*, 2005, **146**, 142–145.

6 H. L. Zhang, C. H. Sun, F. Li, C. Liu, J. Tan and H. M. Cheng, *J. Phys. Chem. C*, 2007, **111**, 4740–4748.
7 S. K. Jeong, M. Inaba and R. Mogi, *Langmuir*, 2001, **17**, 8281–8286.
8 Y. S. Hu and W. H. Kong, *Electrochem. Commun.*, 2004, **6**, 126–131.
9 Z. X. Wang, Y. S. Hu and L. Q. Chen, *J. Power Sources*, 2005, **146**, 51–57.
10 G. H. Wrodnigg, J. O. Besenhard and M. Winter, *J. Electrochem. Soc.*, 1999, **146**, 470–472.
11 B. T. Yu, W. H. Qiu, F. S. Li and L. Cheng, *J. Power Sources*, 2006, **158**, 1373–1378.
12 R. J. Chen, F. Wu, L. Li, Y. B. Guan, X. P. Qiu, S. Chen, Y. J. Li and S. X. Wu, *J. Power Sources*, 2007, **172**, 395–403.
13 J. Li, W. H. Yao, Y. S. Meng and Y. Yang, *J. Phys. Chem. C*, 2008, **112**, 12550–12556.
14 M. J. Frisch, G. W. Trucks, H. B. Schlegel, G. E. Scuseria, M. A. Robb, J. R. Cheeseman, J. A. Montgomery, Jr., T. Vreven, K. N. Kudin, J. C. Burant, J. M. Millam, S. S. Iyengar, J. Tomasi, V. Barone, B. Mennucci, M. Cossi, G. Scalmani, N. Rega, G. A. Petersson, H. Nakatsuji, M. Hada, M. Ehara, K. Toyota, R. Fukuda, J. Hasegawa, M. Ishida, T. Nakajima, Y. Honda, O. Kitao, H. Nakai, M. Klene, X. Li, J. E. Knox, H. P. Hratchian, J. B. Cross, C. Adamo, J. Jaramillo, R. Gomperts, R. E. Stratmann, O. Yazyev, A. J. Austin, R. Cammi, C. Pomelli, J. W. Ochterski, P. Y. Ayala, K. Morokuma, G. A. Voth, P. Salvador, J. J. Dannenberg, V. G. Zakrzewski, S. Dapprich, A. D. Daniels, M. C. Strain, O. Farkas, D. K. Malick, A. D. Rabuck, K. Raghavachari, J. B. Foresman, J. V. Ortiz, Q. Cui, A. G. Baboul, S. Clifford, J. Cioslowski, B. B. Stefanov, G. Liu, A. Liashenko, P. Piskorz, I. Komaromi, R. L. Martin, D. J. Fox, T. Keith, M. A. Al-Laham, C. Y. Peng, A. Nanayakkara, M. Challacombe, P. M. W. Gill, B. Johnson, W. Chen, M. W. Wong, C. Gonzalez and J. A. Pople, *GAUSSIAN 03 (Revision B. 01)*, Gaussian, Inc., Pittsburgh PA, 2003.
15 F. Freeman and H. N. Po, *J. Phys. Chem. A*, 2006, **110**, 7904–7912.
16 M. R. Wagner, P. R. Raimann, A. Trifonova, K.-C. Möller, J. O. Besenhard and M. Winter, *Anal. Bioanal. Chem.*, 2004, **379**, 272–276.
17 H. Ota, T. Sato, H. Suzuki and T. Usami, *J. Power Sources*, 2001, **97–98**, 107–113.
18 H. Ota, T. Akai, H. Namita, S. Yamaguchi and M. Normura, *J. Power Sources*, 2003, **119–121**, 567–571.
19 M. Lu, H. Cheng and Y. Yang, *Electrochim. Acta*, 2008, **53**, 3539–3546.